A straightforward procedure for the synthesis of silica@polyaniline core-shell nanoparticles

Nicolas Roosz, Myriam Euvrard, Boris Lakard, Lydie Viau

A straightforward procedure for the synthesis of silica@polyaniline core-shell nanoparticles

Nicolas Roosz,[a] Myriam Euvrard,[a] Boris Lakard[a] and Lydie Viau[a*]

[a] *Institut UTINAM, UMR CNRS 6213, Univ. Bourgogne-Franche-Comté, Equipe Matériaux et Surfaces Fonctionnels, 16 route de Gray, 25030 Besançon Cedex, France*

* To whom correspondence should be sent: E-mail: lydie.viau@univ-fcomte.fr; Fax: + (33) 3 81 66 62 88; Tel: + (33) 3 81 66 62 93

Abstract

The synthesis of core-shell silica@polyaniline nanoparticles is of interest for many applications including electrorheology and inkjet printing. Formation of such structures by simple adsorption of aniline onto silica surfaces followed by polymerization is rather difficult. Chemical grafting of alkoxysilane monomers on silica surfaces followed by polymerization has been used to prepare silica@polyaniline microspheres but has never been applied to silica nanoparticles. Here, we report an efficient method to prepare silica@polyaniline nanoparticles of different sizes. This study goes far beyond the simple synthetic procedure. It also evidences a general law that can be applied by all to anticipate the efficient encapsulation of silica nanoparticles by polyaniline. Here, silica nanoparticles of different sizes (90 to 300 nm) were firstly synthesized by Stöber process and then functionalized with *N*-[3-(Trimethoxysilyl)propyl]aniline. The last step implied the room temperature polymerization of aniline in the presence of these functionalized-silica nanoparticles using ammonium persulfate as oxidant. Several sets of particles were prepared using different amounts of aniline monomers resulting in different polyaniline thicknesses. SEM, TEM, IR, TGA and XPS were then used to characterize thoroughly these core-shell particles.

The highlight of this paper is that efficient encapsulation of silica particles by polyaniline occurred if, and only if, the ratio between the polyaniline thickness and the particle diameter was close to 10%. Higher ratio led to the presence of isolated polyaniline granules while lower ratio resulted in uncompleted encapsulation.

Keywords

Silica, Polyaniline, Core-shell, Alkoxysilane, Particles

1. Introduction

Since their discovery in the beginning of the 70's, conducting polymers (CPs) including poly(3,4-ethylenedioxydethiophene) (PEDOT), polypyrrole (PPy) and polyaniline (PANI) have been widely used for energy storage, sensors and electrochromic applications.[1-4] In particular, PANI is a non-toxic and low-cost polymer that presents good thermal stability and good conductivity. Different PANI-based composites have been prepared with porous carbon, graphene, carbon nanotubes and metal oxides for application in energy storage conversion,[5] anticorrosion protection,[6-8] microwave absorption,[9, 10] and sensing.[11, 12] Among the

different composites, core-shell particles are the most interesting as the shape is given by the particles core and the properties are driven by the shell. Moreover, after removal of the core, hollow shell structures are obtained and might be of interest for sensing and catalytic applications.[13] Many research groups have investigated the formation of SiO_2@CPs core-shell structure for in inkjet-printing,[14] photonic crystals and electrorheology applications.[15-18] While the synthesis of SiO_2@PEDOT seems straightforward,[19] the formation of SiO_2@PANI or SiO_2@PPy particles is rather more difficult. Armes and collaborators described in 1991 the first synthesis of core-shell structures using micrometer-size silica particles as the core and PANI as the shell. [20] However, despite the use of a low oxidant and monomer concentration to slow the reaction down and to promote polymerization on the surface rather than in the bulk, SEM micrographs have shown that silica particles were not uniformly coated with polyaniline. In two separate reports Jang and collaborators described the formation of SiO_2@PANI core-shell nanoparticles.[21, 22] In the first publication in 2006, particles less than 30 nm in diameter with a thin PANI layer (2 nm) were obtained by controlling the pH of the silica suspension in order to favor electrostatic interactions between anilinium cations and the negatively charged silica surface.[21] We recently reinvestigated the first synthesis of Jang and collaborators and found that core-shell SiO_2@PANI particles cannot be obtained using their procedure. Instead, in accordance with other groups, we confirmed that large silica particles were coated, at least in part, with polyaniline, while the use of small particles led to raspberry-like morphology.[23] In the second paper, the same authors used self-stabilized dispersion polymerization carried out in an aqueous/organic liquid system at -30°C to obtain core-shell particles with diameter ranging from 18 to 130 nm depending on the silica NPs used but thicknesses were not determined.[22] Beside the physical adsorption of PANI onto silica nanoparticles another strategy relies on the *in-situ* or post-synthesis grafting of a polymerizable ligand followed by polymerization to generate the polymer shell.[24] In the case of silica particles, the presence of hydroxy groups on their surface allowed the grafting of polymerizable ligands bearing silanol functions. Among the different alkoxysilanes reported in the literature, 3-aminopropyl(triethoxysilane) (APTS) and *N*-[(3-trimethoxysilyl)-propyl] aniline (TMSPA) have been most widely used for the preparation of SiO_2@PANI particles.[25] Park *et al.* described the synthesis of SiO_2@PANI microspheres to prepare electrorheological material. Silica microspheres of 1µm diameter were coated with TMSPA followed by polymerization in the presence of aniline using ammonium persulfate (APS) as the oxidant. In the resulting microspheres, a PANI shell of about 50 nm was measured by TEM analysis.[26] Yeh and collaborators used the *in-situ*

method to graft TMSPA on silica particles. For this, a co-condensation method was used. Tetraethoxysilane (TEOS) and TMSPA were co-hydrolyzed in the presence of ammonium hydroxide using poly(ethylene glycol) as stabilizer resulting in the formation of silica particles of 720 to 840 nm diameters. Then, the chemical oxidative polymerization of aniline led to PANI thickness of 60-120 nm. In this paper, the main objective was to obtain raspberry-shaped hollow spheres after removal of the silica core by HF etching. These hollow spheres present good conductivities of $1.2\text{-}5.6\times10^{-3}$ $S.cm^{-1}$.[27] These previous studies have shown that it is possible to prepare SiO_2@PANI microspheres. However, for application in catalysis,[28] dyed sensitized solar cells[29] and sensors,[30] smaller core-shell particles presenting higher surface area will be more useful.

In this paper, we report an efficient and simple method for the synthesis of SiO_2@PANI nanoparticles of various diameters (90-300 nm) by grafting of TMSPA on silica surface followed by chemical oxidative polymerization of aniline. The resulting SiO_2@PANI particles have been fully characterized by SEM and TEM observations, FT-IR, TGA and XPS measurements.

2. Experimental section

2.1. Chemicals

The following chemicals were purchased and used as received: tetraethoxysilane 98% (TEOS) and ammonium persulfate (APS) from Acros Organics, ethanol 99.7% from VWR, ammonia 35% and Aniline 99.5% (Ani) from VWR, *N*-[3-(Trimethoxysilyl)propyl]aniline (TMSPA) from Alfa-Aesar.

2.2. Characterization

Morphologies of resulting silica@PANI samples were examined by Scanning Electron Micrography using a HITACHI S4800 FEG HR Scanning Electron Microscope or a FEI Quanta FEG 200 apparatus without previous metallization of the samples. Transmission Electron Microscopy (TEM) observations were carried out at 100 kV (JEOL ARM 200). Samples for TEM measurements were deposited from ethanol solutions on copper grids.

Zeta potential and hydrodynamic sizes of particles were determined at 25°C using a Malvern Zetasizer NanoZS equipped with a He–Ne laser (λ = 632.8 nm). For hydrodynamic size

measurements, the back-scattered mode was used at an angle of 173°. After dilution to 0.5 $g.L^{-1}$ in 10^{-2} $mol.L^{-1}$ NaCl, the silica particles suspensions were sonicated for 2 min before measurement. An equilibration time of 2 min was set before measurement. The cumulant method was used to determine the apparent equivalent hydrodynamic diameters (D_H). Each measurement was performed twice, and the expressed diameter is an average of these two measurements. ζ-potential was calculated using the Smoluchowski approximation. Here again, two measurements were performed to determine the mean ζ-potential values.

Infrared spectra were recorded with a 2 cm^{-1} resolution on a Bruker Vertex70 FTIR spectrometer using a Platinum ATR accessory equipped with a diamond crystal.

Thermogravimetric analysis (TGA) was carried out in an alumina crucible using a TA instruments Q600. Samples were heated under an air flow up to 800 °C with a heating rate of 10 $°C.min^{-1}$

X-ray photoelectron spectroscopy (XPS) spectra were collected on a Versaprobe 5000 (Physical Electronics) equipped with a monochromatic Al Kα (1486.7 eV) source. Analyzed surface had a 200 µm diameter. Shirley method was used to remove the background signal.[31] Photoelectron peaks areas were used to determine the surface atomic concentrations using the atomic sensitivity factors reported by Scofield and corrected by transfer function of analyzer.[32] Binding energies (BE) referred to the C-C/C-H of C1s carbon at 284.8 eV.

2.3. Synthesis

2.3.1. Synthesis of silica particles (Si-OH)

We used our previously reported procedure to synthesize three population of silica particles.[23] Typically, NH_3 was added to a mixture of EtOH and distilled water and the resulting solution was stirred at room temperature for 20 min. The control of the resulting silica particles sizes was achieved using three ammonia concentrations: 1.0, 0.38 and 0.27 $mol.L^{-1}$. After that, TEOS was added dropwise and the resulting mixture was stirred at room temperature for 24h. This led to the formation of a white suspension of colloidal silica. The SiO_2 particles were then centrifuged at 16 000 rpm for 10 minutes and then, washed three times with ethanol and finally with distilled water until the pH of the supernatant reached 8.5-9. Between each washing step, the particles were sonicated. The products were finally dried at 80°C for 16 hours. The amounts of reagents used are given in Table 1.

Table 1. Reagents and quantities used in the preparation of silica particles Si-OH.

Silica particles	D_h (nm)	V_{EtOH} (mL)	V_{H2O} (mL)	V_{NH3} (mL)	V_{TEOS} (mL)
300-SiOH	300	124.4	8.6	8.3	6.6
160-SiOH	160	124.5	8.6	3.3	6.6
90-SiOH	90	132.3	8.6	2.4	6.6

2.3.2. Aniline modified particles (Si-Ani)

To 500 mg of unmodified Si-OH particles suspension dispersed in 42 mL of dried toluene under ultrasound were added appropriate amounts of *N*-[3-(Trimethoxysilyl)propyl]aniline (0.036-0.16 mmol) (TMSPA). The mixture was allowed to reflux overnight under N_2. After cooling down to room temperature, the functionalized Si-Ani particles were then collected by centrifugation during 10 minutes at 16 000 rpm. Here again, they were washed three times with ethanol and deionized water. Each washing step involved a sonication step. To finish, the products were dried at 80°C for 16 hours. The amounts of reagents used are given in Table 2.

Table 2. Quantities of TMSPA used for the preparation of modified silica particles Si-Ani.

Samples	V_{TMSPA} (µL)
300-Si-Ani	8.7
160-Si-Ani	16.2
90-Si-Ani	37.0

2.4. Preparation of core-shell particles SiO_2@PANI

In a typical experiment, 150 mg of functionalized silica particles (Si-Ani) were dispersed in 50 mL of distilled water under ultrasound. After that, aniline was added and the pH was stabilized to 3.5 by addition of small amount of HCl 1.0 mol.L^{-1}. The resulting suspension was stirred for 90 min at room temperature. An aqueous solution of APS oxidant ([APS] = 0.345 mol.L^{-1}) was then added dropwise to the suspension to obtain a ratio [APS]/[Ani] of 1.25. This ratio was chosen after optimization.[23] The reaction mixture was stirred until the end of the polymerization process as observed by the formation of the green color and stabilization of the pH value around 1.5. The particles were recovered by centrifugation, washed four times with ethanol and deionized water and finally dried at 80°C for 16 hours. In Table 3, samples are named *x*-Si@PANI*y* where *x* represents the hydrodynamic diameter (nm) and *y* is the theoretical PANI content (% wt).

Table 3. Quantities of aniline used for the preparation of core-shell SiO_2@PANI particles.

Silica particles	Theoretical PANI content (% wt)	V_{Ani} (µL)	Time
300-Si@PANI65	65	273	16 h
300-Si@PANI30	30	63	16 h
300-Si@PANI10	10	16	7 days
160-Si@PANI84	84	772	16 h
160-Si@PANI49	49	141	16 h
160-Si@PANI20	20	37	16h
90Si@PANI40	40	98	16h
90Si@PANI23	23	43	4 days

3. Results and discussion

3.1. Synthesis and characterization of surface-modified silica particles

The general synthesis procedure followed to prepare the surface functionalized particles and the core-shell particles is summarized in Scheme 1.

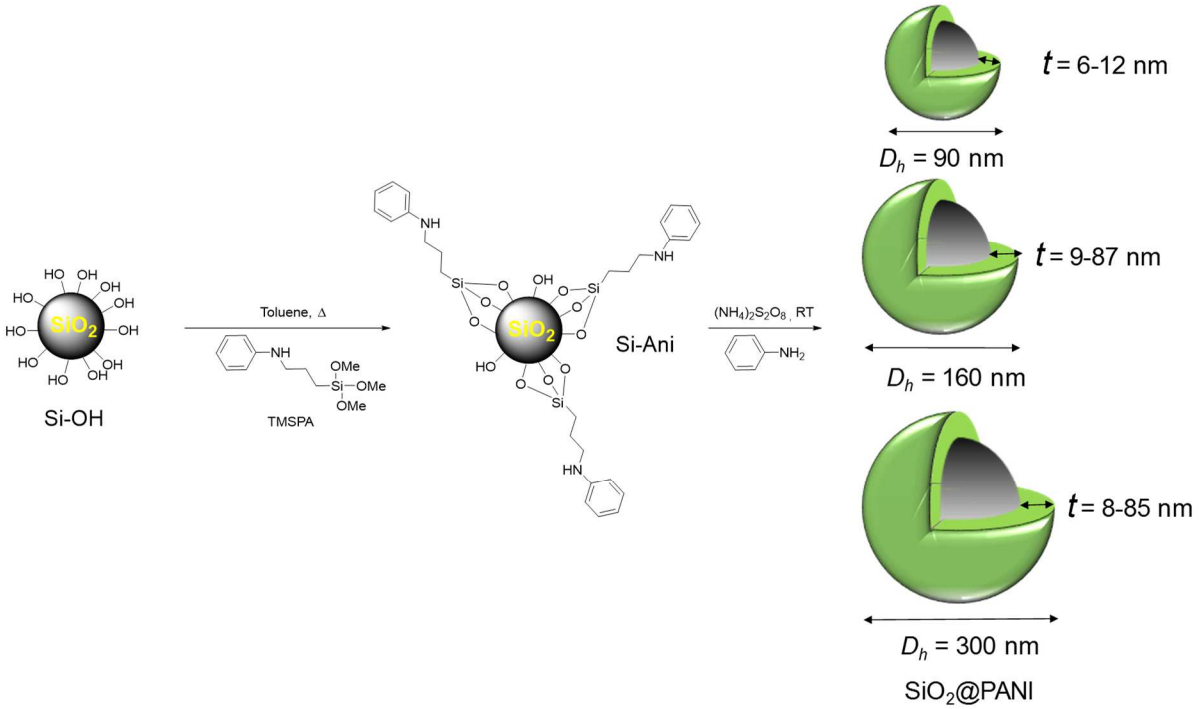

Scheme 1. Strategy used for the synthesis of SiO_2@PANI particles.

Three sizes of silica nanoparticles (Si-OH) were synthesized by sol-gel synthesis according to a procedure described by Stöber *et al.*[33] and Matsoukas and Gulari.[34] *i.e* by hydrolysis of

TEOS in an alcoholic medium in the presence of water and ammonia. For this, three different concentrations of ammonia were used: 1.0, 0.38 and 0.27 mol.L^{-1}. SEM images evidenced the formation of spherical and monodisperse particles (Fig. 1) with mean diameters D_{SEM} of 285 ± 30 nm, 160 ± 30 nm and 80 ± 20 nm (values are based on counting 100 spheres on SEM images). DLS measurements performed on the same particles led to hydrodynamic diameters that were only slightly larger than those obtained by SEM measurements (D_h = 300 ± 70 nm, D_h = 160 ± 70 nm and D_h = 90 ± 15 nm) (Fig.2).

These particles were then functionalized by reaction with *N*-[3-(Trimethoxysilyl)propyl]aniline (TMSPA) in refluxing toluene resulting in the chemical grafting of aniline monomers on the silica surface.

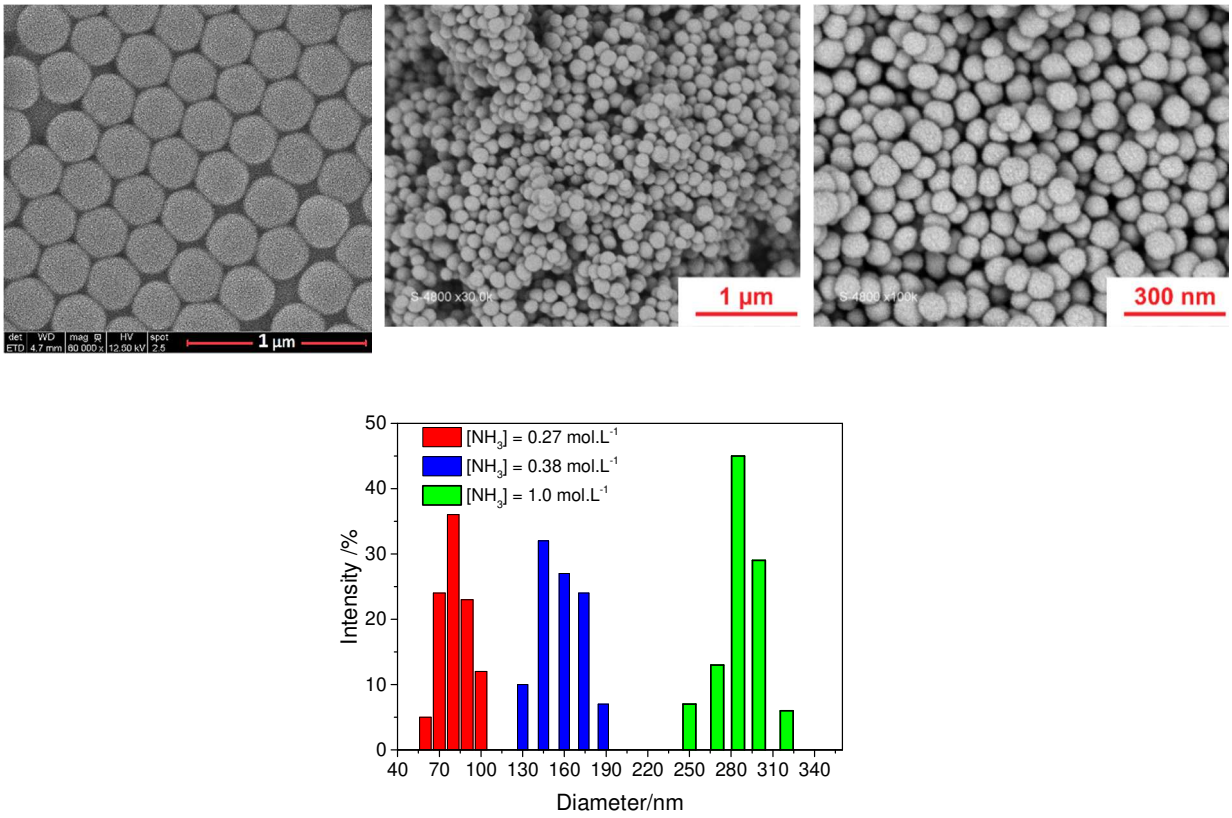

Fig. 1. SEM images of silica particles synthesized using ammonia concentrations of (left) 1.0 mol L^{-1}, (middle) 0.38 mol.L^{-1} and (right) 0.27 mol L^{-1} with their size distribution.

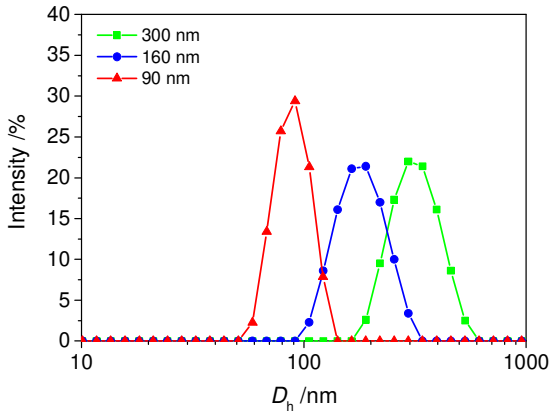

Fig. 2. Particles size distributions of Si-OH particles measured by DLS.

The zeta potential for both functionalized (Si-Ani) and non-functionalized (Si-OH) silica particles was measured at different pH values. As shown in Figure 3, the zeta potential of the Si-OH silica particles is negative for pH value higher than 3 (corresponding to the isoelectric point of silica) due to the deprotonation of silanol groups to form silanolate. The evolution of ζ with pH is the same for the three kinds of functionalized Si-Ani particles investigated. Their surfaces are positively charged at pH below 5.0 and negatively charged for pH values above 6.0. The isoelectric point was thus found around 5.5 in accordance with the pKa of *N*-propylaniline.[35] The surface charges of the functionalized particles are positive at pH<5.0 due to the protonation of the amino functions. This confirmed the efficient functionalization of our particles. At pH above 6, the surface charges become negative and resemble those obtained with unmodified silica meaning. At these pH values, the propylaniline group is neutral and the surface potential is now governed by the presence of remaining silanols functions.

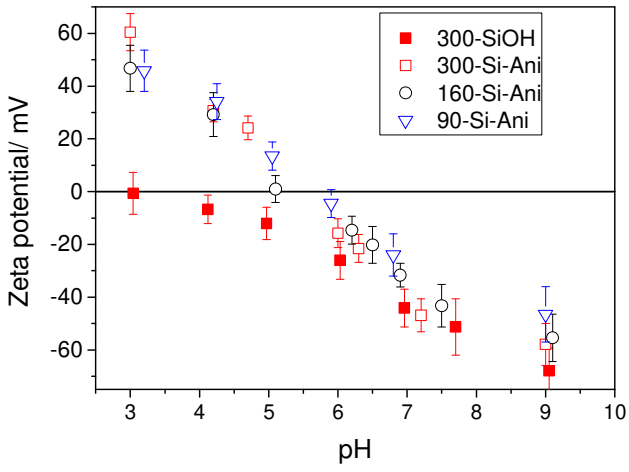

Fig. 3. Zeta potential versus pH for silica particles before and after TMSPA functionalization.

Further surface analysis and TGA measurements were performed on both neat (90-Si-OH) and functionalized SiO_2 particles (90-Si-Ani) of 90 nm diameter presenting the highest surface area. XPS measurements evidenced the surface modification of these particles. (Table 4). Indeed, the survey spectrum of the Si-OH nanoparticles shows Si, O and a minor amount of C, N and Cl elements due to contamination during XPS measurements (Fig. 4). After functionalization of the particles, a decrease of the Si and O contents and an increase of the C content is observed. The carbon-to-nitrogen ratio C:N value of 10.4 is close to the theoretical value of 9.0 if TMSPA molecules were totally hydrolyzed and condensed into silica. The slightly higher ratio found might be due to carbon contamination or to the incomplete hydrolysis of TMSPA.

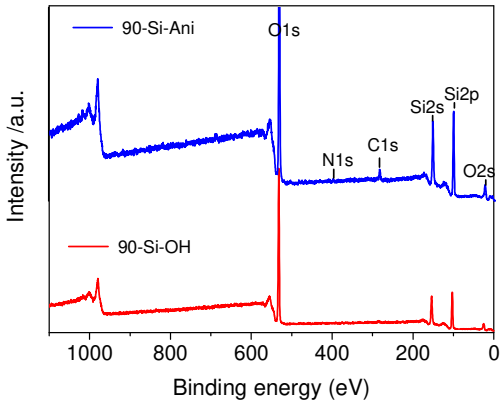

Fig. 4. XPS survey spectra of 90 nm silica particles before and after functionnalization.

Table 4. Surface composition of naked particles and functionalized silica particles as determined by XPS.

Sample	Elemental composition (atomic %)				
	C	N	O	Si	Cl
90-SiOH	1.8	0.3	68.3	29.5	0.2
90-SiAni	5.2	0.5	65.7	28.6	

Fig. 5 represents the TGA traces of Si-OH and Si-Ani silica particles. The first weight loss below 150°C is attributed to the loss of adsorbed water while the weight loss from 150°C up to 800°C is characteristics to the simultaneous decomposition of organic component and the condensation of silanol groups.

The amount of water released during the first step is lower for the functionalized silica in comparison with pristine silica. This is attributable to the presence of grafted TMSPA which renders the silica surface more hydrophobic resulting in lower water adsorption. The weight loss of the functionalized silica in the second stage is slightly larger than that of neat silica due to the presence of grafted TMSPA. The calculation of quantity of grafted TMSPA is based on the weight loss between 150 and 800ºC. The TMSPA grafting density of modified silica (y) was calculated using equation (1) and was estimated to be 1.89×10^{-6} µmol.m^{-2}.

$$y = \frac{\left(\frac{\Delta m2}{Res2} - \frac{\Delta m1}{Res1}\right)}{(M*S)} \text{ (equation 1)}$$

where Δm_2 and Δm_1 represent the weight loss of functionalized and bare silica from 150 to 800°C, respectively. Res_1 and Res_2 refer to the residual weight of the same samples at 800°C. M is the molecular mass of the degradable part of TMSPA which is 134 g.mol^{-1} and S is the specific surface area (S = 67.4 g.mol^{-1}).[23]

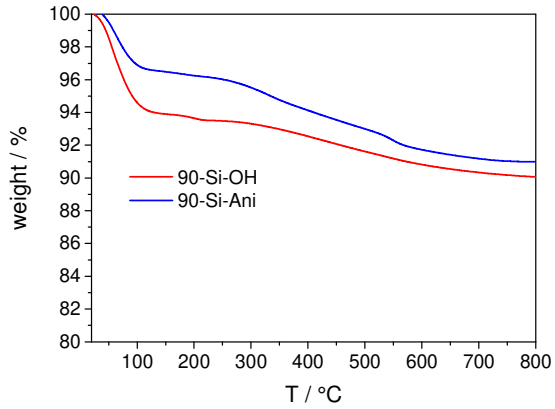

Fig. 5. TGA of the 90 nm silica particles before and after functionalization with TMSPA.

3.2. Synthesis and characterization of SiO_2@PANI particles

3.2.1 Synthesis and morphology

From the three sizes of silica functionalized particles, several sets of experiments were performed in order to prepare core-shell SiO_2@PANI particles. For comparison purpose, we performed the polymerization in the same experimental conditions as described before.[23] Therefore, we used ammonium persulfate as the oxidant, the oxidant to monomer ratio was fixed to 1.25, the starting pH value to 3.5 and the reactions were performed at room temperature. The end of aniline polymerization was followed by pH. Thus, we considered that the polymerization was finished when the pH value was stable and close to 1.5. In Table 5 are summarized all experiments performed with the three NPs sizes. A first series was prepared

with the 300-Si-Ani particles with the objectives to incorporate 65, 30 and 10 wt% of PANI (samples 300-Si@PANI65, 300-Si@PANI30 and 300-Si@PANI10) corresponding to thicknesses *t* of 85.1, 27.5 and 8.1 nm, respectively, which were evaluated with the following equation:[36]

$$t = R\left[\sqrt[3]{\left(\frac{wt\%_{PANI}\times\rho_{SiO2}}{wt\%_{SiO2}\times\rho_{PANI}}+1\right)}-1\right] \text{ (equation 2)}$$

where *t* is the polyaniline overlayer thickness, *R* is the radius of the silica particles, $wt\%_{PANI}$ and $wt\%_{SiO2}$ are the mass fraction of PANI and SiO_2, respectively, ρ_{SiO2} and ρ_{PANI} are the density of silica (ρ_{SiO2} = 2.04 g.cm^{-3})[37] and PANI (ρ_{PANI} = 1.33 g.cm^{-3}).[38]

In the second sets of experiments, we used 160-Si-Ani particles and kept these thicknesses constant resulting in samples containing 84, 49 and 20 wt% polyaniline (small differences in thicknesses between 300-Si particles and 160-Si particles are due to the fact that values have been calculated based on the real amount of aniline introduced). In the last sets of experiments, using 90-Si-Ani particles, we expected these thicknesses to be too high compared to the particles size and have thus decided to study only two *t* values of 11.9 and 5.9 nm representing 10 and 22 wt% of polyaniline.

In table 5 are also summarized the ϕ value calculated as being the ratio between the theoretical thickness *t* and the hydrodynamic diameter of silica particles D_h.

Table 5. Theoretical and experimental PANI content and thicknesses in the PANI@SiO_2 particles.

Samples	D_h (nm)	PANI content (%wt)		*t* (nm)		ϕ[d] (%)
		Theor[a]	Exp[b]	Theor[a]	Exp[c]	
300-Si@PANI65	300	65	nd	85.1	nd	28.4
300-Si@PANI30	300	30	27.7	27.5	25 ± 4	9.1
300-Si@PANI10	300	10	10.1	8.1	6 ± 3	2.7
160-Si@PANI84	160	84	nd	86.7	nd	54.2
160-Si@PANI49	160	49	nd	28.2	nd	17.6
160-Si@PANI20	160	20	18.7	9.1	10 ± 2	11
90-Si@PANI40	90	40	nd	11.9	nd	27
90-Si@PANI23	90	22	22.0	5.9	7 ± 2	13

[a] theoretical values determined from equation (2);[b] experimental values determined by TGA; [c] experimental values determined from TEM images; [d] $\phi = t/D_h*100$

The morphology of the resulting particles was determined by SEM (Figure 6). Sample 300-Si@PANI65 contains clearly a mixture of PANI granules and PANI@SiO_2 particles while samples 160-Si@PANI84, 160-Si@PANI49 and 90-Si@PANI40 present particles that are glue together. Stejskal and collaborators have demonstrated that polymerization of aniline in the presence of silica surfaces occurred preferentially on the silica surface rather than in bulk solution.[39] Later on, the same group has also shown that smaller particles, with higher surface area, led to less amount of precipitated PANI particles.[40] Based on their results, our observations can be explained as follow: in the presence of silica particles with low surface area and a high aniline content (sample 300-Si@PANI65), polymerization occurs first on the silica surface but the excess of aniline monomer in solution is high enough to lead to the formation of PANI granules. Using particles with higher surface area, the polymerization of aniline in the bulk is suppressed and the polymerization occurs only on the particles surfaces. However, in the presence of high aniline content, PANI chains grow further and are prone to interact with each other's leading to particles gluing (samples 160-Si@PANI84, 160-Si@PANI49 and 90-Si@PANI40). For the other samples, the encapsulation looks rather homogeneous. From these first observations, we can conclude at a first approximation, that only ϕ values below 15% result in the formation of core-shell particles.

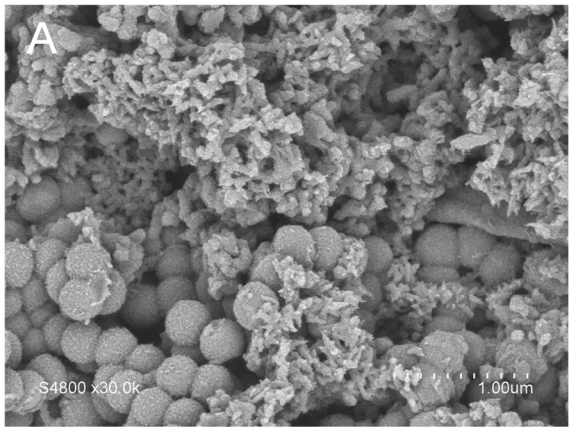

300-Si@PANI65

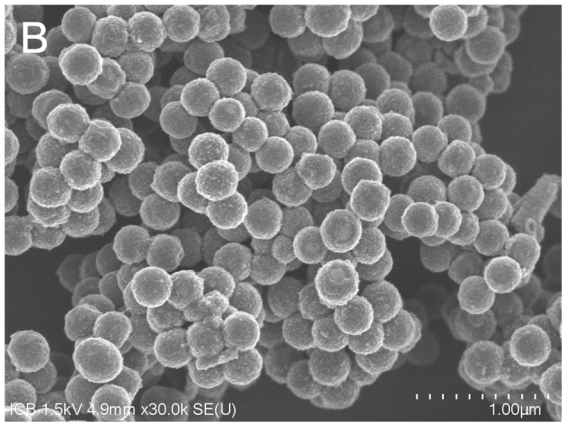

300-Si@PANI30

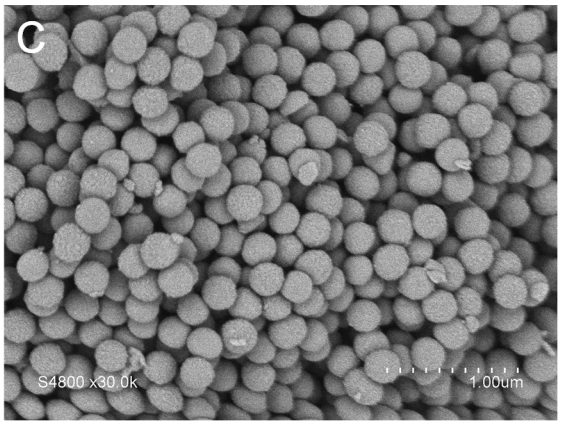

300-Si@PANI10

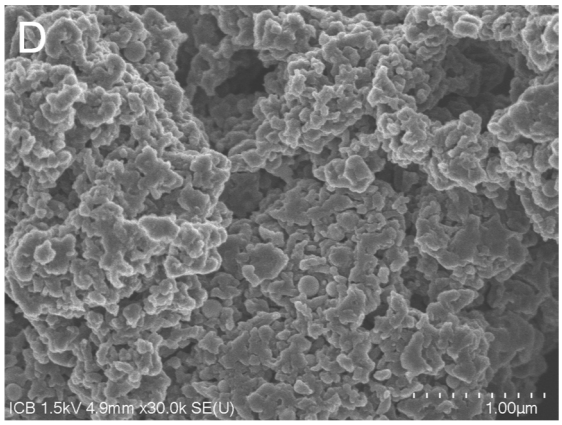

160-Si@PANI84

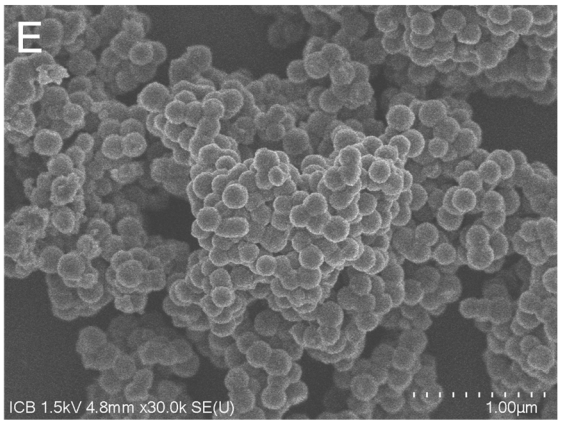

160-Si@PANI49

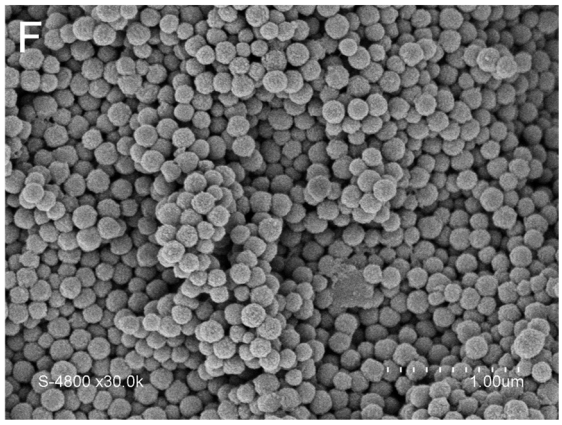

160-Si@PANI20

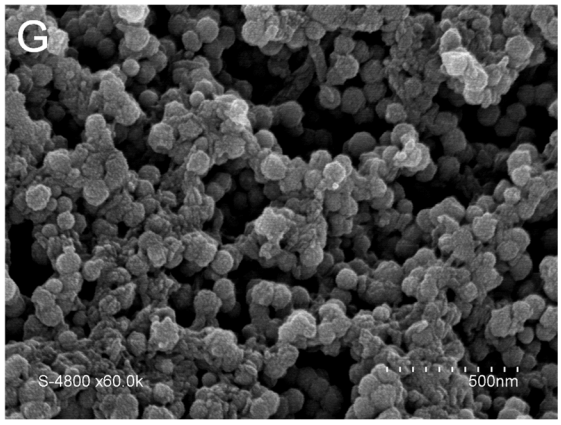

90-Si@PANI40

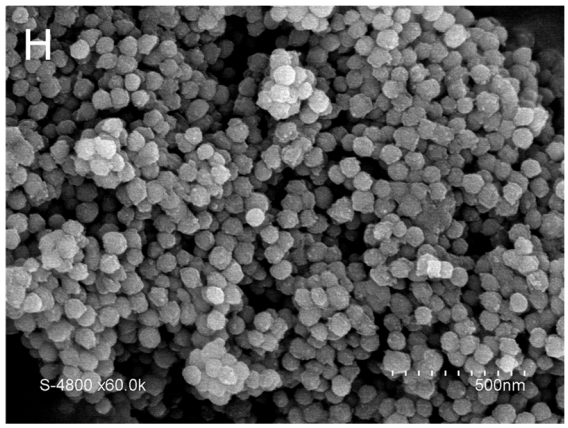

90-Si@PANI23

Fig. 6. SEM images of the SiO_2@PANI particles.

In order to observe the core-shell structure for the four remaining samples with $\phi < 15\%$, TEM measurements were performed as shown in Figure 7. In all cases, the core-shell structure is confirmed. Thicknesses were determined on these TEM images and the resulting values are reported in Table 5. These values agree very well with the theoretical ones confirming the efficient formation of the core-shell structures.

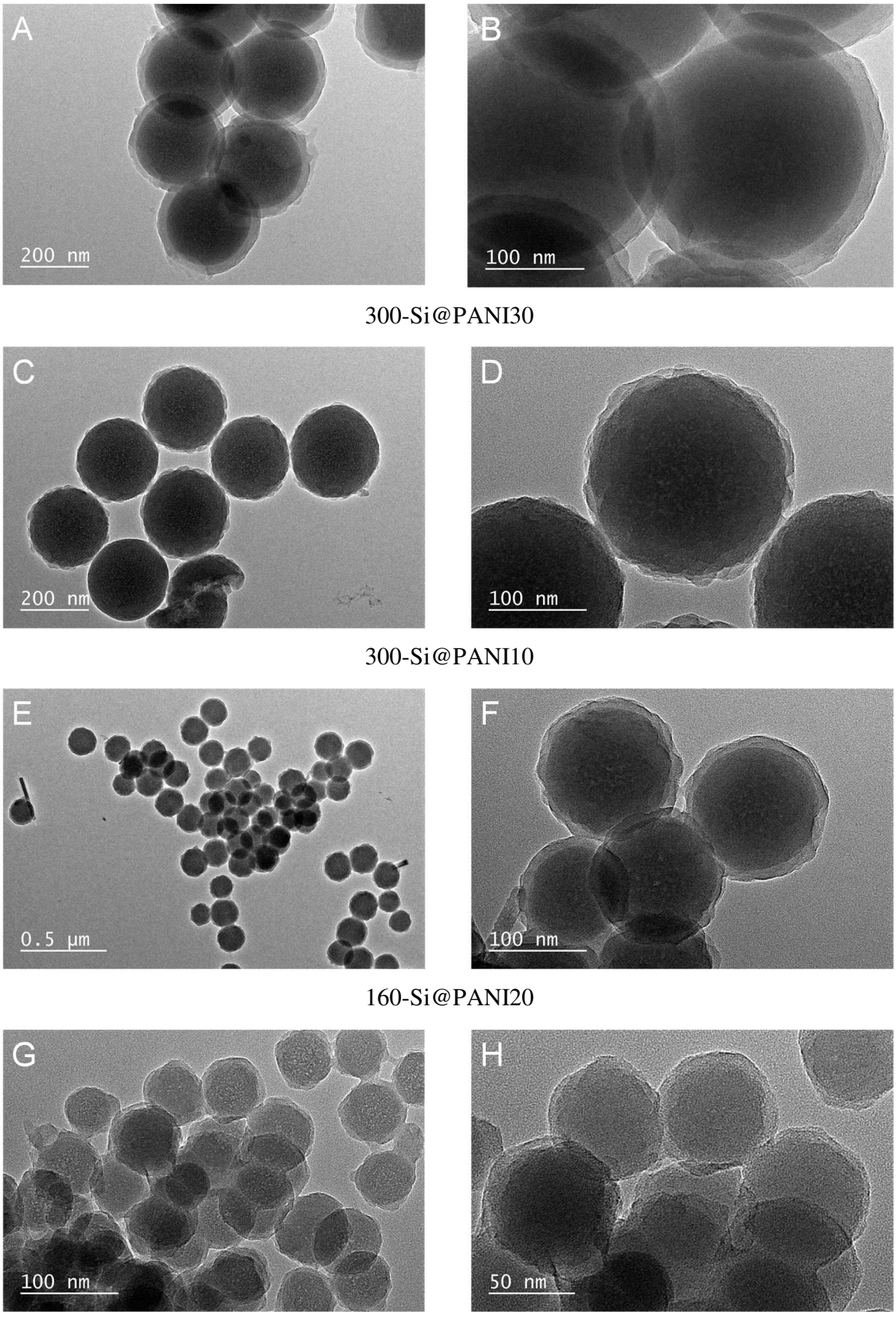

Fig. 7. TEM images of the SiO_2@PANI particles.

3.2.2. Infrared spectroscopy

Fig. 8 illustrates the ATR-IR spectra of SiO_2@PANI particles, silica and PANI. The spectrum of naked colloidal SiO_2 particles shows four characteristic absorption bands at 1065, 950, 795 and 450 cm^{-1} attributable to asymmetric vibration of Si-O-Si siloxane bonds, asymmetric vibration of Si-OH, symmetric vibration of Si-O-Si and racking mode of Si-O-Si, respectively.[41] The spectra of the SiO_2@PANI particles look rather the same but contain also bands characteristic to the presence of polyaniline in its emeraldine salt form. Indeed, bands of the quinoid (Q) and benzenoid (B) rings are clearly visible in the region 1570–1590 and 1480–1500 cm^{-1}, respectively. In the 1200-1350 cm^{-1} region, a band at 1300–1310 cm^{-1} and a shoulder at 1220 cm^{-1} are characteristics of the C-N stretching of secondary aromatic amine and to the C-NH^+ stretching.[42-44]. The presence of polyaniline is also confirmed by the presence of C-H bands at 860–880, 690–700, and 570–580 cm^{-1}. The presence of silica-PANI interactions is evidenced by a shift to higher wavenumbers of the bands located at 1490 and 1587 cm^{-1}. The most important shift is obtained for 300-Si@PANI30 sample ($\Delta\nu$ = 18 and 50 cm^{-1}) and the lowest shift is obtained for samples 300-Si@PANI10 ($\Delta\nu$ = 10 and 2 cm^{-1}). Such shifts have been observed previously by other groups and have been attributed to hydrogen bonding between remaining silanols groups on silica and the π-electron cloud of the PANI phenyl groups.[42, 44-46] Based on this, the highest shift found for 300-Si@PANI30 is characteristic to highest silica-PANI interactions.

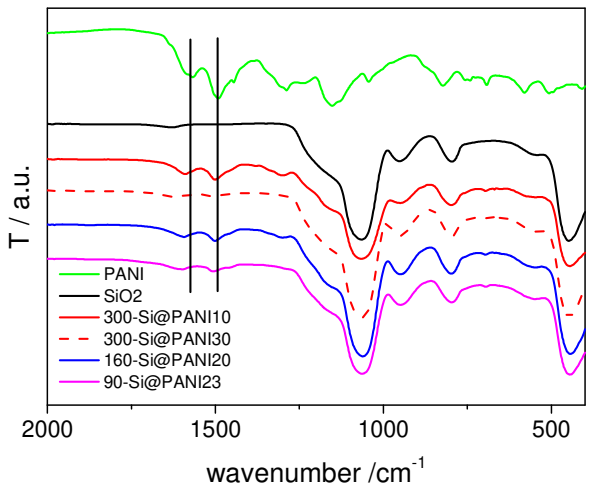

Fig. 8. ATR-IR spectra of resulting SiO_2@PANI particles.

3.2.3. Thermogravimetric analysis

The polyaniline contents in the core-shell particles was determined by thermogravimetric analyses under air up to 800°C. The temperatures of decomposition corresponding to a 5% loss of the total mass are given in Table 5. The thermogravimetric traces depicted in Figure 9 show that thermal profiles of core-shell particles present two main losses. The first one occurs below 100°C and is attributed to the loss of absorbed water while the second decomposition step occurs from 350°C to 700°C and is attributed to the decomposition of polyaniline. At 800°C, only the inorganic silica part of the particles remains. Based on this, the PANI content can be determined from the weight loss occurring in the second step. As expected, the experimental PANI contents correspond well with the theoretical ones (See Table 5).

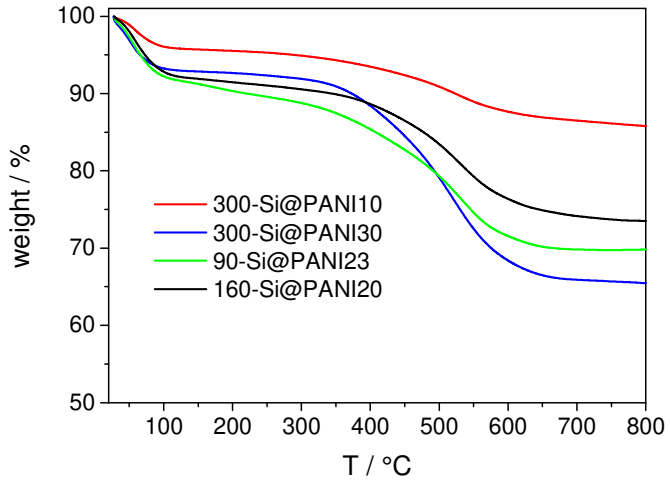

Fig. 9. TGA traces of SiO_2@PANI particles under air flow (rate: 10 °C.min^{-1}).

3.2.4. XPS measurements

The surface chemistry of the SiO_2@PANI particles was investigated by XPS, and the resulting atomic compositions (in at%) are shown in Table 6. As expected, the incorporation of PANI shell around the silica particles results in an increase of both the C and N contents with a concomitant decrease of Si and O contents. The presence of a small amount of chlorine atoms is also detected due to the use of HCl to reduce the pH to 3.5 to perform the polymerization. This also means that PANI is in its doped state and contains Cl^- counter-anions. A strong decrease of the Si/N ratio is also observed after polymerization for the core-shell particles. In the case of sample 300-Si@PANI10, this ratio is relatively high (Si/N = 6.28) suggesting an incomplete encapsulation. This result is somehow surprising compared to the conclusion made based on SEM and TEM observations showing uniform PANI shell. A possible explanation for these discrepancies might come from the fact that the PANI thickness

(≈ 6 nm) is close to the X-Ray penetration depth or might be accounted to the SEM and TEM observations which are not representative to a whole sample. For the other samples, the ratio Si/N is much lower showing an efficient encapsulation and even reaches a value of 0.42 for the sample 300-Si@PANI30 that presents the highest thickness of 25 nm. Interestingly these results can be linked to the shift observed in IR spectra. Indeed, the sample 300-Si@PANI10 presenting the highest Si/N ratio shows the lowest IR shifts while sample 300-Si@PANI30 that presents the lowest Si/N ratio was the one with the highest IR shift (see above).

Note that our multiple attempts to prepare compressed pellets for conductivity measurements failed. Indeed, the prepared core-shell particles contain a very high amount of silica which renders the pellets very fragile.

Table 6. Surface composition of PANI and SiO_2@PANI particles as determined by XPS.

Sample	Elemental composition (atomic %)						
	C	N	O	Si	Cl	S	Si/N
PANI	75.1	11.8	10.6	0.3	0.8	1.4	0.03
90-Si-Ani	5.2	0.5	65.7	28.6	-	-	57.20
300-Si@PANI30	71.1	9.7	13.8	4.1	0.8	0.5	0.42
300-Si@PANI10	28.6	3.2	46.2	20.1	-	nd	6.28
160-Si@PANI20	58.3	7.9	23.8	8.7	0.6	nd	1.10
90-Si@PANI23	40.7	5.3	36.5	13.7	0.5	nd	2.58

3. Conclusions

In this paper, we report an easy procedure to prepare SiO_2@PANI nanoparticles of different diameters. The synthesis starts with the functionnalization of synthesized silica particles with *N*-[(3-trimethoxysilyl)-propyl] aniline followed by chemical oxidative polymerization of aniline at room temperature. The resulting core-shell particles have been carefully characterized by TGA, IR, SEM, TEM and XPS analysis thus eluding any doubts about the formation of the core-shell structures. Interestingly, based on our results, we draw a general guide for those who may be interested in the synthesis of SiO_2@PANI nanoparticles. First, based on SEM observations we demonstrate that formation of PANI granules and PANI-Silica composites that are glue together can be avoid if the ratio ϕ between the particle thickness and its diameter is kept below 15%. These first assumptions have been confirmed by TEM observations from which theoretical thicknesses were measured and agreed well with

theoretical ones. A more detailed study of the SiO_2@PANI nanoparticles surface by XPS analysis finally shows that, when this ϕ value is too low, the encapsulation is not total. In this case, the amount of polyaniline is not high enough to cover the whole particles surface. For an efficient encapsulation, a reasonable ϕ value that can be used is 10%. This study may inspire other authors interested in the elaboration of different core-shell nanoparticles based on an organic part and an inorganic one.

Acknowledgements

N.R. thanks the Ministère de l'Enseignement Supérieur et de la Recherche for a PhD scholarship. We are thankful to Dr. Olivier Heintz from the Laboratoire interdisciplinaire Carnot de Bourgogne (UMR-CNRS 6303, France) for carrying out the XPS measurements described in this study.

References

[1] A.G. MacDiarmid, "Synthetic metals": A novel role for organic polymers (Nobel lecture), Angew. Chem. Int. Ed. 40(14) (2001) 2581-2590.
[2] G.A. Snook, P. Kao, A.S. Best, Conducting-polymer-based supercapacitor devices and electrodes, J. Power Sources 196(1) (2011) 1-12.
[3] U. Lange, N.V. Roznyatouskaya, V.M. Mirsky, Conducting polymers in chemical sensors and arrays, Anal. Chim. Acta 614(1) (2008) 1-26.
[4] P.M. Beaujuge, J.R. Reynolds, Color Control in pi-Conjugated Organic Polymers for Use in Electrochromic Devices, Chem. Rev. 110(1) (2010) 268-320.
[5] H. Wang, J. Lin, Z.X. Shen, Polyaniline (PANi) based electrode materials for energy storage and conversion, J. Sci. Adv. Mater. Devices 1(3) (2016) 225-255.
[6] C.H. Chang, T.C. Huang, C.W. Peng, T.C. Yeh, H.I. Lu, W.I. Hung, C.J. Weng, T.I. Yang, J.M. Yeh, Novel anticorrosion coatings prepared from polyaniline/graphene composites, Carbon 50(14) (2012) 5044-5051.
[7] S. Radhakrishnan, C.R. Siju, D. Mahanta, S. Patil, G. Madras, Conducting polyaniline-nano-TiO_2 composites for smart corrosion resistant coatings, Electrochim. Acta 54(4) (2009) 1249-1254.
[8] P.P. Deshpande, N.G. Jadhav, V.J. Gelling, D. Sazou, Conducting polymers for corrosion protection: a review, J. Coat. Technol. Res. 11(4) (2014) 473-494.
[9] C.L. Yuan, Y.S. Hong, Microwave adsorption of core-shell structure polyaniline/SrFe12O19 composites, J. Mater. Sci. 45(13) (2010) 3470-3476.
[10] J. Yun, J.S. Im, H.-I. Kim, Y.-S. Lee, Effect of oxyfluorination on electromagnetic interference shielding of polyaniline-coated multi-walled carbon nanotubes, Colloid. Polym. Sci. 289(15-16) (2011) 1749-1755.
[11] D.W. Hatchett, M. Josowicz, Composites of intrinsically conducting polymers as sensing nanomaterials, Chem. Rev. 108(2) (2008) 746-769.
[12] L. Al-Mashat, K. Shin, K. Kalantar-zadeh, J.D. Plessis, S.H. Han, R.W. Kojima, R.B. Kaner, D. Li, X. Gou, S.J. Ippolito, W. Wlodarski, Graphene/Polyaniline Nanocomposite for Hydrogen Sensing, J. Phys. Chem. C 114(39) (2010) 16168-16173.

[13] R. Panigrahi, S.K. Srivastava, Ultrasound assisted synthesis of a polyaniline hollow microsphere/Ag core/shell structure for sensing and catalytic applications, RSC Advances 3(21) (2013) 7808-7815.
[14] G.H. Shim, M.G. Han, J.C. Sharp-Norton, S.E. Creager, S.H. Foulger, Inkjet-printed electrochromic devices utilizing polyaniline-silica and poly(3,4-ethylenedioxythiophene)-silica colloidal composite particles, J. Mater. Chem. 18(5) (2008) 594-601.
[15] T.L. Kelly, M.O. Wolf, Template approaches to conjugated polymer micro- and nanoparticles, Chem. Soc. Rev. 39(5) (2010) 1526-1535.
[16] J. Trlica, P. Saha, O. Quadrat, J. Stejskal, Electrorheology of polyaniline-coated silica particles in silicone oil, J. Phys. D: Appl. Phys. 33(15) (2000) 1773-1780.
[17] A. Lengalova, V. Pavlinek, P. Saha, J. Stejskal, T. Kitano, O. Quadrat, The effect of dielectric properties on the electrorheology of suspensions of silica particles coated with polyaniline, Phys. A 321(3-4) (2003) 411-424.
[18] Y.D. Liu, F.F. Fang, H.J. Choi, Silica nanoparticle decorated conducting polyaniline fibers and their electrorheology, Mater. Lett. 64(2) (2010) 154-156.
[19] M.G. Han, S.H. Foulger, Preparation of poly(3,4-ethylenedioxythiophene) (PEDOT) coated silica core-shell particles and PEDOT hollow particles, Chem. Commun. (19) (2004) 2154-2155.
[20] S.P. Armes, S. Gottesfeld, J.G. Beery, F. Garzon, S.F. Agnew, Conducting polymer colloidal silica composites, Polymer 32(13) (1991) 2325-2330.
[21] J.S. Jang, J. Ja, B. Lim, Synthesis and characterization of monodisperse silica-polyaniline core-shell nanoparticles, Chem. Commun. (15) (2006) 1622-1624.
[22] M. Kim, S. Cho, J. Song, S. Son, J. Jang, Controllable Synthesis of Highly Conductive Polyaniline Coated Silica Nanoparticles Using Self-Stabilized Dispersion Polymerization, ACS Appl. Mater. Interfaces 4(9) (2012) 4603-4609.
[23] N. Roosz, M. Euvard, B. Lakard, C.C. Buron, N. Martin, L. Viau, Synthesis and characterization of polyaniline-silica composites: Raspberry vs core-shell structures. Where do we stand?, J. Colloid Interface Sci. 502 (2017) 184-192.
[24] S.A. Jadhav, V. Brunella, D. Scalarone, Polymerizable Ligands as Stabilizers for Nanoparticles, Part. Part. Syst. Char. 32(4) (2015) 417-428.
[25] Y.Z. Dong, W.J. Han, H.J. Choi, Polyaniline Coated Core-Shell Typed Stimuli-Responsive Microspheres and Their Electrorheology, Polymers 10(3) (2018) 299-331.
[26] D.E. Park, H.J. Choi, V. Cuong Manh, Stimuli-responsive polyaniline coated silica microspheres and their electrorheology, Smart Mater. Struct. 25(5) (2016) 055020-055031.
[27] C.-F. Dai, C.-J. Weng, C.-M. Chien, Y.-L. Chen, S.-Y. Yang, J.-M. Yeh, Using silane coupling agents to prepare raspberry-shaped polyaniline hollow microspheres with tunable nanoshell thickness, J. Colloid Interface Sci. 394 (2013) 36-43.
[28] A.A. Yelwande, M.E. Navgire, B.R. Arbad, M.K. Lande, Polyaniline/SiO_2 Nanocomposite Catalyzed Efficient Synthesis of Quinoxaline Derivatives at Room Temperature, J. Chin. Chem. Soc. 59(8) (2012) 995-1000.
[29] P. Ma, J. Tan, H. Cheng, Y. Fang, Y. Wang, Y. Dai, S. Fang, X. Zhou, Y. Lin, Polyaniline-grafted silica nanocomposites-based gel electrolytes for quasi-solid-state dye-sensitized solar cells, Appl. Surf. Sci. 427 (2018) 458-464.
[30] C.-J. Weng, Y.-L. Chen, C.-M. Chien, S.-C. Hsu, Y.-S. Jhuo, J.-M. Yeh, C.-F. Dai, Preparation of gold decorated SiO_2@polyaniline core–shell microspheres and application as a sensor for ascorbic acid, Electrochim. Acta 95 (2013) 162-169.
[31] D.A. Shirley, High-Resolution X-Ray Photoemission Spectrum of the Valence Bands of Gold, Phys. Rev. B 5(12) (1972) 4709-4714.
[32] J.H. Scofield, Hartree-Slater subshell photoionization cross-sections at 1254 and 1487 eV, J. Electron. Spectrosc. Relat. Phenom. 8(2) (1976) 129-137.

[33] W. Stöber, A. Fink, E. Bohn, Controlled growth of monodisperse silica spheres in the micron size range, J. Colloid Interface Sci. 26(1) (1968) 62-69.
[34] T. Matsoukas, E. Gulari, Dynamics and growth of silica particles from ammonia-catalyzed hydrolysis of tetraethylorthosilicate, J. Colloid Interface Sci. 124(1) (1988) 252-261.
[35] H.C. Brown, D.H. McDaniel, O. Häfliger, Chapter 14 - Dissociation Constants, in: E.A. Braude, F.C. Nachod (Eds.), Determination of Organic Structures by Physical Methods, Academic Press1955, pp. 567-662.
[36] S.F. Lascelles, S.P. Armes, Synthesis and characterization of micrometre-sized, polypyrrole-coated polystyrene latexes, J. Mater. Chem. 7(8) (1997) 1339-1347.
[37] G.H. Bogush, M.A. Tracy, C.F. Zukoski, Preparation of monodisperse silica particles - control of size and mass fraction, J. Non-Cryst. Solids 104(1) (1988) 95-106.
[38] J. Stejskal, R.G. Gilbert, Polyaniline. Preparation of a conducting polymer (IUPAC technical report), Pure Appl. Chem. 74(5) (2002) 857-867.
[39] S. Fedorova, J. Stejskal, Surface and precipitation polymerization of aniline, Langmuir 18(14) (2002) 5630-5632.
[40] J. Stejskal, M. Trchova, S. Fedorova, I. Sapurina, J. Zemek, Surface polymerization of aniline on silica gel, Langmuir 19(7) (2003) 3013-3018.
[41] G.D. Chukin, V.I. Malevich, Infrared spectra of silica, J. Appl. Spectrosc. 26 (1977) 223-229.
[42] G. Ciric-Marjanovic, L. Dragicevic, M. Milojevic, M. Mojovic, S. Mentus, B. Dojcinovic, B. Marjanovic, J. Stejskal, Synthesis and Characterization of Self-Assembled Polyaniline Nanotubes/Silica Nanocomposites, J. Phys. Chem. B 113(20) (2009) 7116-7127.
[43] J. Stejskal, I. Sapurina, M. Trchova, E.N. Konyushenko, Oxidation of aniline: Polyaniline granules, nanotubes, and oligoaniline microspheres, Macromolecules 41(10) (2008) 3530-3536.
[44] X.M. Feng, G. Yang, Y.G. Liu, W.H. Hou, J.J. Zhu, Synthesis of polyaniline/MCM-41 composite through surface polymerization of aniline, J. Appl. Polym. Sci. 101(3) (2006) 2088-2094.
[45] Z.W. Niu, Z.H. Yang, Z.B. Hu, Y.F. Lu, C.C. Han, Polyaniline-silica composite conductive capsules and hollow spheres, Adv. Funct. Mater. 13(12) (2003) 949-954.
[46] Y.F. Li, J.Y. Li, X.H. Gao, S. Qi, J. Ma, J.J. Zhu, Synthesis of stabilized dispersion covalently-jointed SiO2@polyaniline with core-shell structure and anticorrosion performance of its hydrophobic coating for Mg-Li alloy, Appl. Surf. Sci. 462 (2018) 362-372.

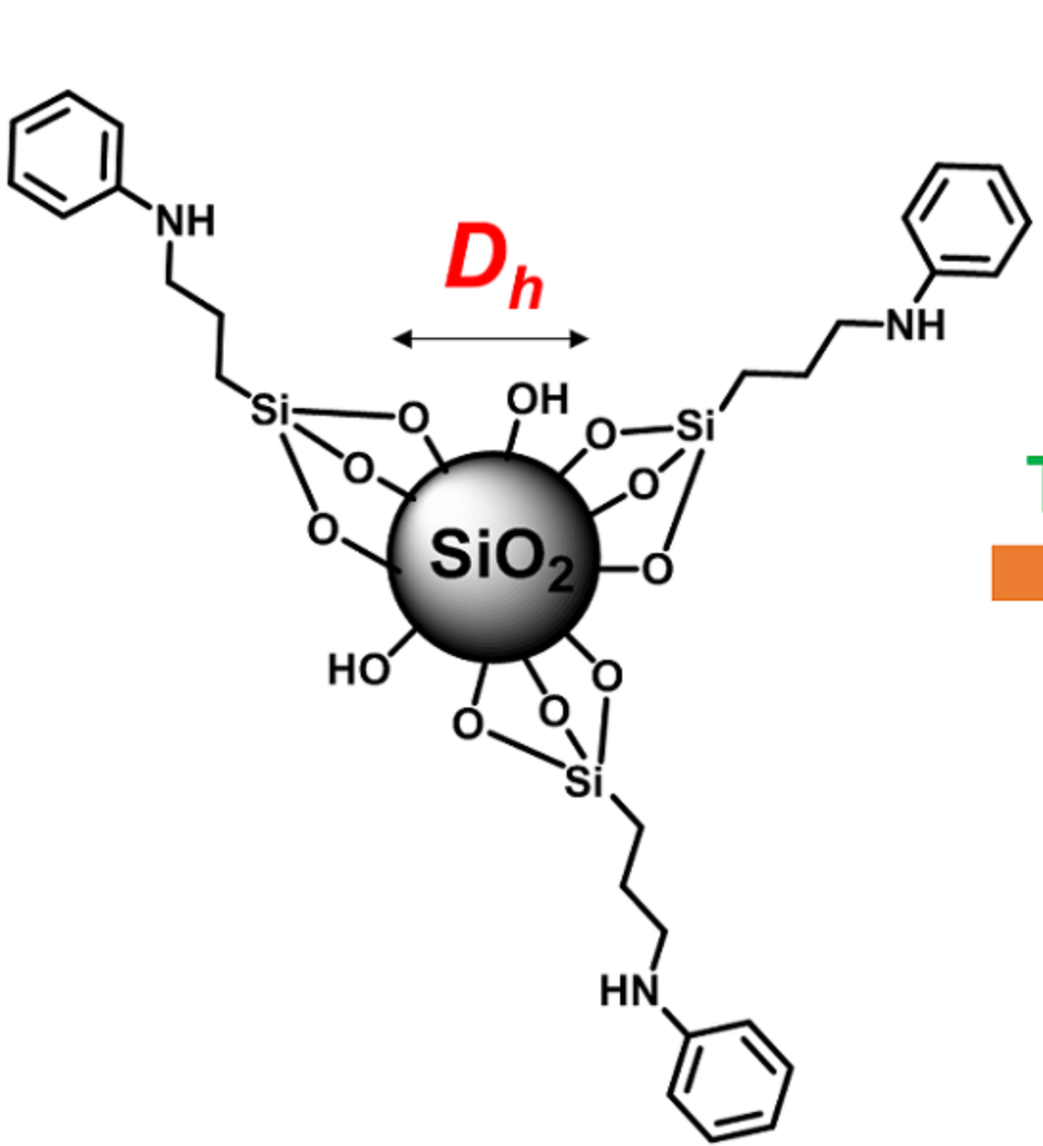

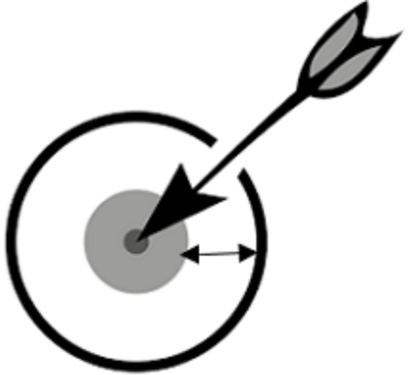

Target thickness *t*

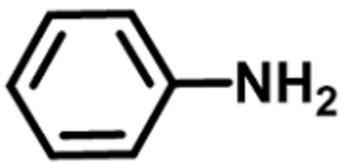

$\Phi = t/D \approx 10\%$

SiO_2@PANI